

AperTO - Archivio Istituzionale Open Access dell'Università di Torino

Cyclodextrins as a Templating Agent in Solvent-Free Kneading- Based Syntheses of Nanosized SnO₂ and ZnO

This is a pre print version of the following article:

Original Citation:

Availability:

This version is available <http://hdl.handle.net/2318/1874582> since 2022-10-04T13:23:30Z

Published version:

DOI:10.1021/acssuschemeng.2c02344

Terms of use:

Open Access

Anyone can freely access the full text of works made available as "Open Access". Works made available under a Creative Commons license can be used according to the terms and conditions of said license. Use of all other works requires consent of the right holder (author or publisher) if not exempted from copyright protection by the applicable law.

(Article begins on next page)

1 Cyclodextrins as templating agent in solvent-free
2 kneading-based syntheses of Nanosized SnO₂ and
3 ZnO

4 *Alberto Rubin Pedrazzo^{a*}, Andrea Jouve^a, Sara Morandi^a, Maela Manzoli^b, Claudio Cecone^a,*
5 *Pierangiola Bracco^a and Marco Zanetti^{a,c}*

6

7 ^aDepartment of Chemistry, University of Torino, Via P. Giuria 7, NIS and INSTM Reference
8 Centres University of Torino, 10125 Torino, Italy

9 ^bDepartment of Drug Science and Technology, NIS and INSTM Reference Centres University of
10 Torino, Via Giuria 9, 10125 Torino, Italy

11 ^cICxT Centre, University of Torino, Lungo Dora Siena 100, 10153 Torino, Italy

12

13 KEYWORDS

14 Kneading, cyclodextrins, MOS, semiconductor metal oxides, mechanochemistry

15 ABSTRACT

16 -----

17 INTRODUCTION

18 In recent years, gas sensors have been increasingly used in industrial production and daily life:
19 efficient, low cost and small-sized sensors are nowadays requested in many fields of applications
20 such as environmental, food or biomedical [REF].

21 In this context, in the ultra-sensible sensors field there has been a growing interest and diffusion
22 of metal oxide-based semiconductors (MOS): MOS are suitable materials for sensors for their
23 outstanding physical and chemical properties that combine high efficiency, fast response, stability
24 and, last but not least, simple preparation and low cost.^{1,2}

25 In gas sensing applications (and in solar cell and photo-catalysis as well) MOS activity is strongly
26 related to the specific surface area^{3,4}. To improve the properties of MOS and, consequentially, to
27 improve efficiency of semiconductor metal oxides-based devices, research is nowadays moving
28 towards nano-sized structures with controllable crystalline phases.

29 There are many examples of synthetic methods for obtaining ceramic nanoparticles, such as
30 thermal and physical deposition, hydro/solvo-thermal processes^{5,6} and, over the last few years,
31 electrospinning (ES)⁷⁻¹⁴.

32 ES is a widespread and relatively simple technique to obtain both micro and nano fibers of
33 polymers usually showing high porosity and high specific surface area¹⁵⁻¹⁷. Recently^{18,19}, our
34 research group adopted the procedure of electrospinning of polymeric solutions containing
35 precursors of ceramics, followed by thermal treatment, for the obtaining of ceramic nanofibers.

36 The addition of an oxide precursors to the ES solutions and a subsequent thermal treatment, above
37 the thermal degradation of the polymer, will ablate the polymer and, at the same time, convert the
38 precursor in the respective oxide^{10,20-22}. Our last work in this field was focused on the influence of
39 the polymer on morphology and microstructure¹⁸, confirming the concept of the polymer as a

40 templating agent, but also as variable capable of influencing morphological properties and the size
41 of the final oxide particles. In this work we are proposing a new synthetic route of nanosized MOS,
42 based on the same combination of oxide precursors and polymers (in this case oligomers) as
43 templating agent, exploiting a more simple and fast approach that does not involve an
44 electrospinning step. The ES, before calcination, is indeed replaced by the simple kneading of the
45 precursors in presence of an excess of cyclodextrins.

46 Cyclodextrins (CDs) are a family of cyclic oligosaccharides, composed of α -D-glucopyranose
47 units linked through α -1,4 glycosidic bonds, with a peculiar toroidal structure²³. CDs are obtained
48 from enzymatic conversion of starch and are renewable and eco-friendly materials. Moreover CDs
49 are biocompatible and biologically degradable²⁴⁻²⁶. The three major and relevant from the
50 industrial point of view representatives of CDs family are the α -CD, β -CD and γ -CD and are
51 composed of 6, 7 and 8 glucopyranose units, respectively.^{24,26-28}. The CDs structure, with the
52 presence of a slightly apolar cavity and a hydrophilic external part, determines the ability to
53 establish specific interactions with various types of molecules through the formation of
54 noncovalently bonded complexes, either in the solid phase or in aqueous solution. There are many
55 examples in literature of CDs complexes with many different organic compounds^{24,27,29,30} or metal
56 ions^{31,32} and cyclodextrins are extensively used in a wide range of applications^{26,33}.

57 In 2016³⁴, Zhang *et al.* employed host-guest inclusion complexes as versatile (the chemical
58 composition of host-guest inclusion complexes can be finely tuned) precursors for obtaining
59 hetero-doped carbon materials.

60 The present work demonstrates the possibility to exploit inclusion complexes of CDs and metal
61 precursors to obtain nanostructured oxide: cyclodextrins plays in this case the role of a sacrificial
62 template. We selected precursors of SnO₂ and ZnO (two MOS traditionally obtained in form of

63 nanostructures via sol-gel synthesis or, as said, more recently, via electrospinning) because they
64 have been widely investigated in solar cells, photocatalysts and gas sensors^{6,19,35,36}: the inclusion
65 complexes were prepared using Zinc Oxide (ZnAc) and Tin (II) - ethylexanoate (SnEx) and
66 exploiting a sustainable and solvent-free approach, completely based on the simple kneading of α -
67 CD, β -CD and γ -CD and precursors in ball mill.

68 According to the Green Chemistry Principles, published in 1998 by Anastas *et al.*, chemical
69 processes must be designed in order to “minimize the quantity of final waste and to avoid
70 hazardous or toxic solvents”.^{37,38} Unfortunately, toxic solvents are present in most of processes:
71 the recovery and reuse are often expensive, and the disposal is a major concern. Even if in much
72 smaller quantities, the process reported in our previous article¹⁸ for obtaining oxides with
73 electrospinning also involves the use of dimethylformamide for the preparation of the polymeric
74 solution to be electrospun.

75 The use of kneading for the preparation of inclusion complexes with CDs is quite established,
76 permitting to overcome all the limitations related to poorly soluble or insoluble compounds^{29,39,40};
77 in our case permitted to completely avoid the use of solvents and to speed-up the preparation of
78 the MOS precursor.

79 The complexes after kneading were characterized by thermogravimetric analyses and,
80 subsequently, thermally treated for the obtaining of the oxide. After the synthesis the so obtained
81 SnO₂ and ZnO nanoparticles were characterized by scanning electronic microscopy (SEM), high-
82 resolution transmission electron microscopy (HR-TEM) and by X-ray diffraction (XRD) and by
83 measuring the BET surface area, evidencing a possible influence of the CDs dimension on the
84 finale oxide.

85

86 EXPERIMENTAL

87 *Materials*

88 β -CD were provided by Roquette Frères (Lestrem, France) with purity > 95%. α -CD, γ -CD
89 (research grade, purity > 95.0%) were purchased from Cyclolab (Budapest, Hungary) .

90 Cyclodextrins were dried in oven at 75 °C up to constant weight, before use.

91 SnO₂ and ZnO precursors, respectively Tin(II) 2-ethylhexanoate (SnEx, purity grade of 94.4%)
92 and Zinc Acetate (dihydrate, ZnAc), were purchased from Sigma-Aldrich (Steinheim, Germany)
93 and used without further purifications.

94

95 *Ball Mill (BM)*

96 The ball mill used for the kneading step was a Retsch PM200 High Speed Planetary Ball Mill
97 (Haan, Germany), with planetary configuration and Zirconia jars, inner volume 50 mL.

98

99 *Thermogravimetric analyses*

100 Thermogravimetric Analyses (TGA) were performed on a TA Instruments (New Castle, DE, USA)
101 Hi-res Q500 Thermogravimetric Analyzer. TG Analyses parameters are the same for all samples:
102 100 mL/min air-flow, heating rate 10 °C/min, RT to 700 °C. The thermograms were elaborated
103 using TA Instruments Universal Analysis 2000 software and, subsequently, OriginLab2019b.

104

105

106

107

108 *Preparation of the samples*

109 The preparation is the same for all oxides samples and can be divided in 2 parts:

110

111 *Kneading*: an appropriate amount of cyclodextrins (dried powder) is kneaded with the precursor,
112 approximately respecting the molar ratio 2:1, expressing an excess of cyclodextrins.

113 For Tin(II) 2-ethylhexanoate (viscous liquid): 3 g of α -CD, kneaded with 0.624 g of SnEx; 3 g of
114 β -CD, kneaded with 0.535 g of SnEx; 4 g of γ -CD, kneaded with 0.624 g of SnEx.

115 For Zinc Acetate (powder): 3 g of α -CD, kneaded with 0.338 g of ZnAc; 3 g of β -CD, kneaded
116 with 0.290 g of ZnAc; 4 g of γ -CD, kneaded with 0.338 g of ZnAc.

117

118 The mixtures are kneaded for 1 h at 300 rpm. The size of the balls is 5 mm (declared diameter).

119 Approximately 12 mL (volume, measured with graduated cylinder) of sintered zirconium oxide
120 balls, 5 mm of diameter, in each jar. Quantities of kneaded reactants are optimized for this specific
121 volume of balls and, consequently free volume in the jars.

122

123 *Calcination/Elimination of Organic Fraction*: after calcination all samples were thermally treated
124 to eliminate the cyclodextrin matrix and convert the precursor into the correspondent oxide.

125 In a typical procedure approximately 8-10 g of mixture cyclodextrin/precursor contained in a
126 Coors combustion boat were inserted in a Lenton (Hope, UK) tubular furnace.

127 Parameters were optimized via Thermogravimetric Analyses; used conditions were the following:

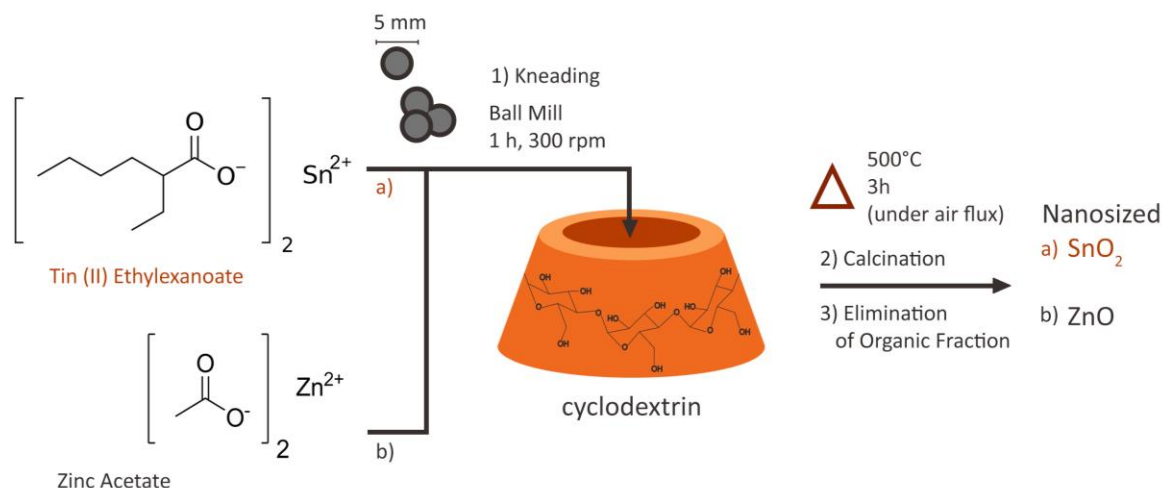
128 3h, 500° C, under 100 mL/min air-flow.

129 A white powder was obtained from all thermal treatments.

130

131 Scheme 1, following, shows a schematic representation of the complete procedure.

132 Further details of the synthesis will be discussed more in deep in the next sections (Results and
133 Discussion).



149 measurements, the samples were outgassed at 100 °C under vacuum (10 mm Hg) for 15 hours (for
150 removing water and eventual adsorbates). The specific surface areas were determined through the
151 Brunauer-Emmett-Teller (BET) method to the adsorption/desorption isotherms of N₂ at 77 K.

152

153 *SEM*

154 Morphological characterization of the samples was performed by scanning electron microscopy
155 (SEM), using a Tescan VEGA 3 SEM (Brno, Czech Republic) working with secondary electrons
156 and 10keV accelerating voltage. The samples were analyzed without any previous metal coating.

157

158 *TEM*

159 High-resolution transmission electron microscopy (HR-TEM) was utilized to achieve further
160 morphological and structural information: the instrument is a Jeol (Akishima, Tokyo, Japan) JEM
161 3010 UHR (300 kV, LaB6 filament). The synthesized samples were deposited on a Cu grid, coated
162 with a porous carbon film. All digital micrographs were acquired by an Ul-traSscan 1000 camera,
163 and the images were processed by Gatan digital micro-graph (Pleasanton, CA, US) .

164

165

166

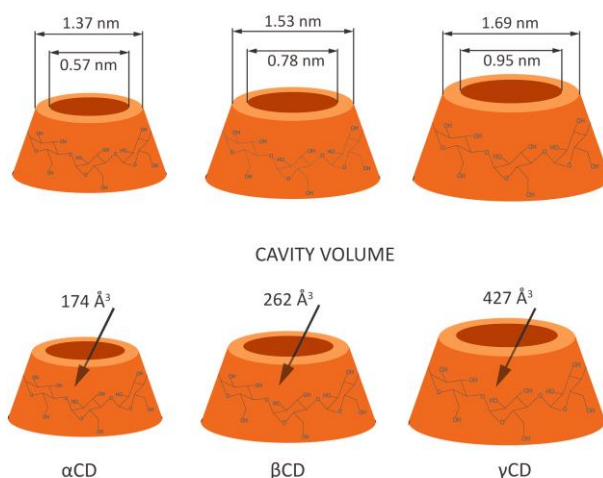
167

168

169 RESULTS AND DISCUSSION

170 The starting point for this project is the idea of using a polymer as a sacrificial template to obtain
171 very small oxide particles for specific applications. The focus is therefore on the final resulting

172 oxide but, as we recently demonstrated ¹⁸, the influence of the polymer on the precursor conversion
173 is dramatic. The choice of the templating polymer, consequentially, is of primary importance. Our
174 choice fell on cyclodextrins for different reasons: CDs are a widely studied oligomer ²⁵, with an
175 extensive literature that supports many of our claims, CDs are a renewable because obtained from
176 enzymatic conversion of starch ^{24,25}. Thus, CDs are renewable, eco-friendly materials and, last but
177 not least, cheap. In Figure 1, following, are reported a simplified chemical structure of a α , β and
178 γ CDs and the respective dimensions of the CDs employed in the present work.



179

180 **Figure 1 - Simplified structure and dimensions of α , β and γ cyclodextrins**

181

182 α , β and γ cyclodextrins exhibit a different size and a different cavity volume (Figure 1, details).

183 The principle behind exploiting CDs as a sacrificial “container” is also associated the relatively

184 high degradation temperature of the pristine CDs, that is roughly around 300°C for α , β and γ

185 cyclodextrins: this is a crucial parameters, because the polymer “matrix”, in this case the oligomer,

186 needs to be completely removed in an efficient way, but still needs to protect e to assist in a

187 synergic way the formation of the oxide. In order to obtain the SnO₂ and ZnO, it is necessary to

188 achieve the complete volatilization of the polymer and the degradation organic precursor ¹⁹. An

189 incomplete elimination of the organic fraction will lead to a grey/black powder, with an amorphous
 190 carbon residue. At the same time, a high temperature can affect the final size of the oxide, which
 191 could favor crystal growth during calcination rather than nucleation, leading to bigger particle and
 192 lower surface area. In Table 1, following, are reported all the synthetic information and the BET
 193 surface area, [m²/g]. A careful correlation of the results shown in Table 1 with the thermal
 194 measurements shown in Figure 2 and Figure 3 (and with data already present in literature), allows
 195 us to make some assumptions.

196

197 **Table 1 – Oxides (α , β and γ SnO₂ and α , β and γ ZnO), relative preparative conditions (kneading step and**
 198 **subsequent thermal treatment) and BET Surface Area (m²/g)**

OXIDE		Precursor	Kneading	Thermal Treatment	BET Surface Area [m ² /g]
SnO ₂	α -SnO ₂	Tin (II) ethylhexanoate	1 h 300 rpm 5,0 mm \varnothing balls 10 min inversion time	3 h 500°C ramp 10 °C/min	44,2
	β -SnO ₂				47,1
	γ -SnO ₂				50,4
ZnO	α -ZnO	Zinc Acetate	1 h 300 rpm 5,0 mm \varnothing balls 10 min inversion time	3 h 500°C ramp 10 °C/min	12,0
	β -ZnO				10,5
	γ -ZnO				17,5

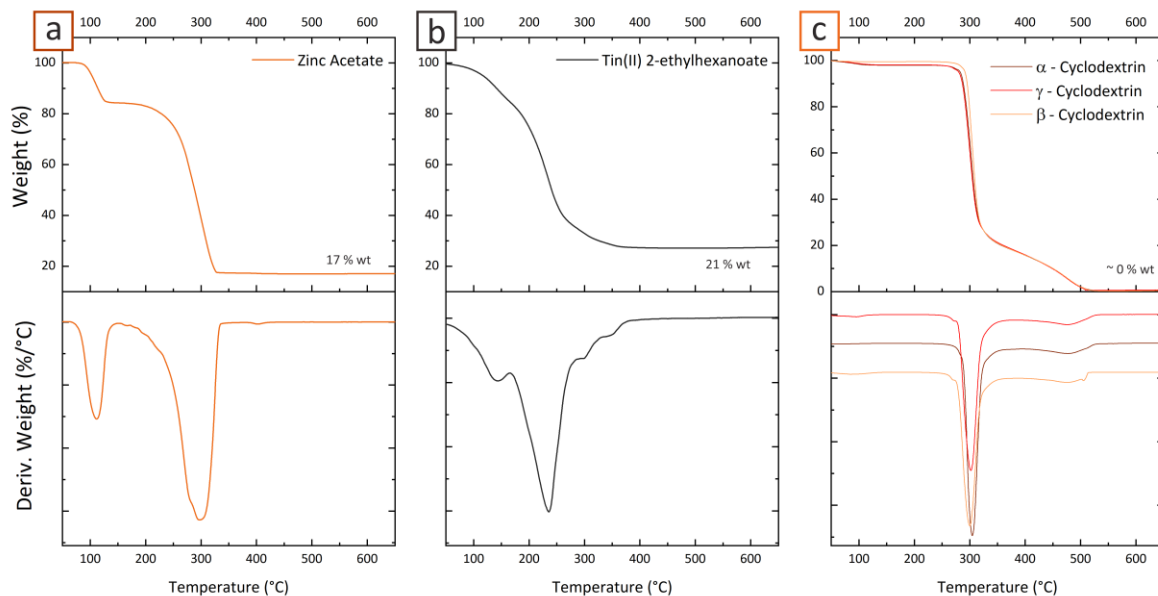
199

200 As shown in Table 1, the preparative conditions are the same for all samples: nevertheless,
 201 outcomes are quite different. The BET Surface area for what concerns the SnO₂ is comprised
 202 between \approx 44 and 50 m²/g, for all CDs template, a quite interesting result, comparable with the
 203 results reported in the literature with oxides and similar treatments REF. It is necessary to
 204 underline, however, that these very interesting results were obtained through an objectively very
 205 simple preparation, without complex procedures and, even more noteworthy, without any solvent

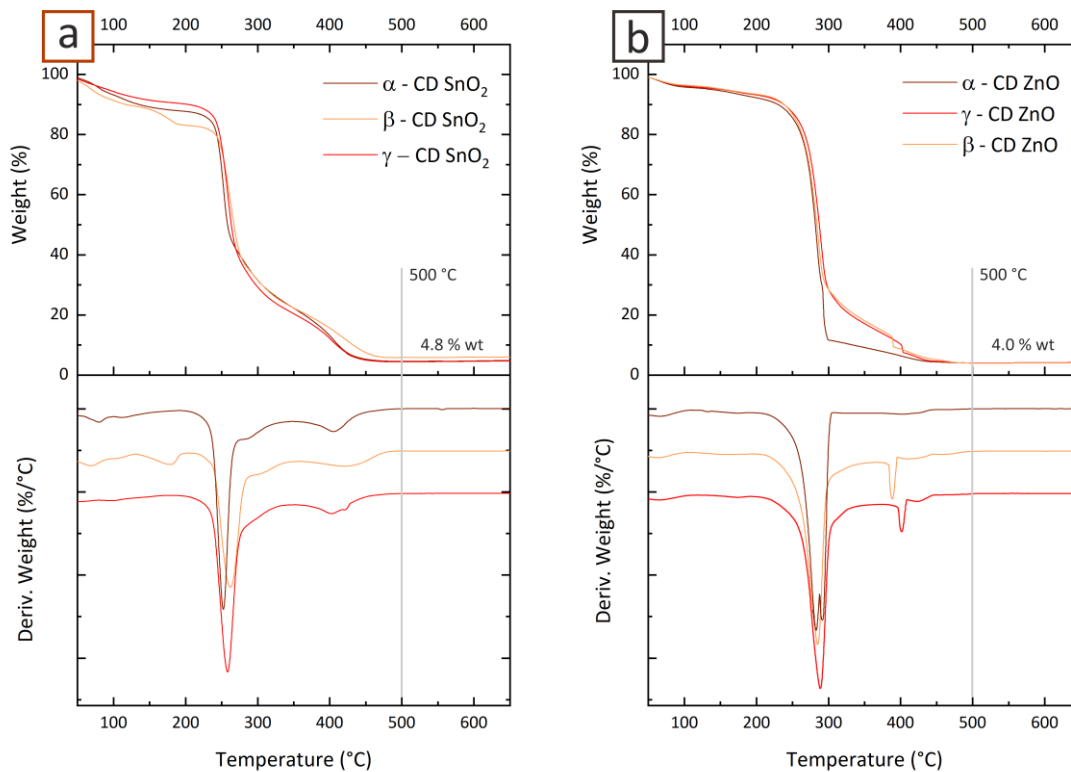
206 in any step. However, the same reasoning cannot be made with regard to ZnO. The oxide obtained
207 has a much lower surface area, indeed. SnO₂ and ZnO are certainly two completely different oxides
208 but the dramatic difference in the final result is clear. Still, the presence of a trend in both oxides
209 from different precursors is evident: the surface area appears to be (with the sole exception of β -
210 ZnO, Table 1 for reference) inversely proportional to the size of the cyclodextrin cavity. It is worth
211 to say that the formation of an inclusion complex is not the only possible way of CDs to form
212 complexes: stable interactions are sometimes established between a guest molecule and the
213 external part of CDs. Indeed, hydroxy group on the outer surface of cyclodextrins can lead to the
214 formation of hydrogen bonds and, consequentially, to water-soluble complexes, in a similar way
215 to what is seen with non-cyclic oligo or polysaccharides^{27,41}. These supramolecular assemblies
216 (there are no covalent bonds) are called *non-inclusion* complexes. They can, eventually, protect
217 guest molecules from the environment and achieve anyway an efficient increase of solubility. In
218 literature many examples of non-inclusion compounds are reported⁴²⁻⁴⁵. Among the others there
219 is, of course, the size compatibility between host and guest molecules. The size of CD has to be
220 large enough to permit the guest entrance but if the guest is too small if compared to the cavity,
221 CD-guest interactions will be very weak, and the dissociated form will prevail on the associated
222 one. The same applies for the opposite situation: a molecule larger than the cavity will enter
223 partially or will arrange outside the cavity. An example in literature is, for example, the
224 naphthalimide, where the apolar chain fit preferentially in a smaller α -cyclodextrin cavity, wherein
225 the aromatic moiety of the same molecule will arrange inside a β -cyclodextrin⁴⁶.

226 It is therefore possible to hypothesize that there is not the real formation of a 1: 1 complex, but
227 rather the formation of “clusters”. Given the interesting results these clusters are necessarily of
228 small size; thus, it is possible to assume that in any case the ion or the precursor are, statistically,

229 partially or completely incorporated by the cyclodextrins and this is more probable with the γ CD,
230 whereas the cavity is larger. This hypothesis can also be supported by a possible interpretation of
231 the thermogravimetric analyses, Figure 2 and Figure 3, following.



232
233 **Figure 2 - Comparison of thermo-gravimetric analysis (TGA) and derivative TGA (DTGA) of the different**
234 **component of the precursor mixture in air, from RT to 700 °C, 10 °C/min. Respectively a) Zinc Acetate b) Tin**
235 **(II) ethylhexanoate c) α , β and γ Cyclodextrins**



236

237 **Figure 3 - Comparison of thermo-gravimetric analysis (TGA) and derivative TGA (DTGA) of α , β and γ SnO₂ from Tin (II) ethylhexanoate/CDs and α , β and γ ZnO from Zinc**
 238 **Acetate/CDs**
 239

240

241 In Figure 2, the thermo-gravimetric analyses and derivative TGA of the different component of
 242 the precursor mixture in air, from RT to 700 °C, are reported. The degradation of ZnAc, inset a)
 243 Figure 2, shows a thermal degradation that proceeds in two different steps: the first one at 100°C
 244 reasonably related to the water and the second one, that starts before 300°C and that leads to a
 245 residue of 17%, can be related to the decomposition of ZnAc itself, that is only partially converted
 246 into ZnO (ZnAc is reported to sublime at 234 °C⁴⁷). Assuming a total conversion of the precursor
 247 into ZnO the residual should amount to approximately 37% wt. A similar situation is shown with
 248 the Tin (II) ethylhexanoate, inset b) Figure 2, where the residue from TG is around 21%: also in this
 249 case the expected quantity of residue, with a complete conversion of the precursor in SnO₂, is 37%.

250 In both precursors, there is a competition between degradation and oxidation, indeed. A different
251 situation is shown in Figure 2, inset c), concerning CDs. The degradation can be divided in three
252 stages⁴⁸: the first one, below 100°C, due to loss of absorbed water and water of crystallization (in
253 this case, since CDs were dried for at least 24h, the weight loss is barely detectable), the second,
254 that develops in a temperature range that start at roughly 250 °C, which is associated with a weight
255 loss of 70-80%, with the formation of a char residue and the third, at $T > 300$ °C, that leads to
256 complete oxidation (combustion) of the residue.

257 The final residue, after the third stage, is $\approx 0\%$ for all cyclodextrins. Cyclodextrins alone, therefore,
258 in an oxidizing atmosphere, do not leave any residue.

259 Consequentially, looking at the thermogram reported in Figure 3, showing a residue around 4.8 %
260 for SnO₂ and 4.0 % for ZnO, it is possible to state that the simultaneous presence of CDs and
261 precursor leads to the formation of an oxide and that the cyclodextrins are completely eliminated
262 from the mixture above 450 °C. In both thermograms, inset a) and b) Figure 3, most of the weight
263 loss profile is related to the volatilization of the cyclodextrin matrix, and this is consistent with
264 what it was possible to hypothesize considering the initial composition of the mixture after
265 kneading. What is necessary to highlight is the amount of residual oxide, because it could confirm
266 a protective effect of the cyclodextrins: the theoretical residue in oxide, assuming a total
267 conversion of the precursor present in the post-kneading mixture is 4.5 % for ZnO and 5.6 % for
268 SnO₂, respectively. Thus, results are remarkably close to the 4.0 % and 4.8 % reported before. The
269 yield is low, but we must consider that the precursor/CDs kneaded mixture contains approximately
270 15% wt. of precursor: tin (II) 2-ethylhexanoate and zinc acetate, if heated in the same conditions,
271 volatilize, leaving a considerably smaller amount of residue, while in this case the precursor is
272 almost completely converted into oxide.

273 Cyclodextrins, therefore, do not only play a role of simple support but rather protect and assist the
274 formation of oxide (preventing the volatilization of the precursor), influencing both its yield and
275 final size.

276 However, it is necessary to make further considerations, about the possible reasons why the same
277 interesting results, concerning the BET surface area (and consequentially particle size) were not
278 obtained as for SnO₂ with ZnO. In Figure 2 it is evident that cyclodextrins have their principal
279 weight loss at a temperature comparable to that of zinc acetate, while it is about 50 °C higher than
280 that of tin (II) 2-ethylhexanoate: given the results previously commented and assuming therefore
281 that there is a protective effect, this is effective only if the “shield” molecule does not degrade
282 before the host molecule.

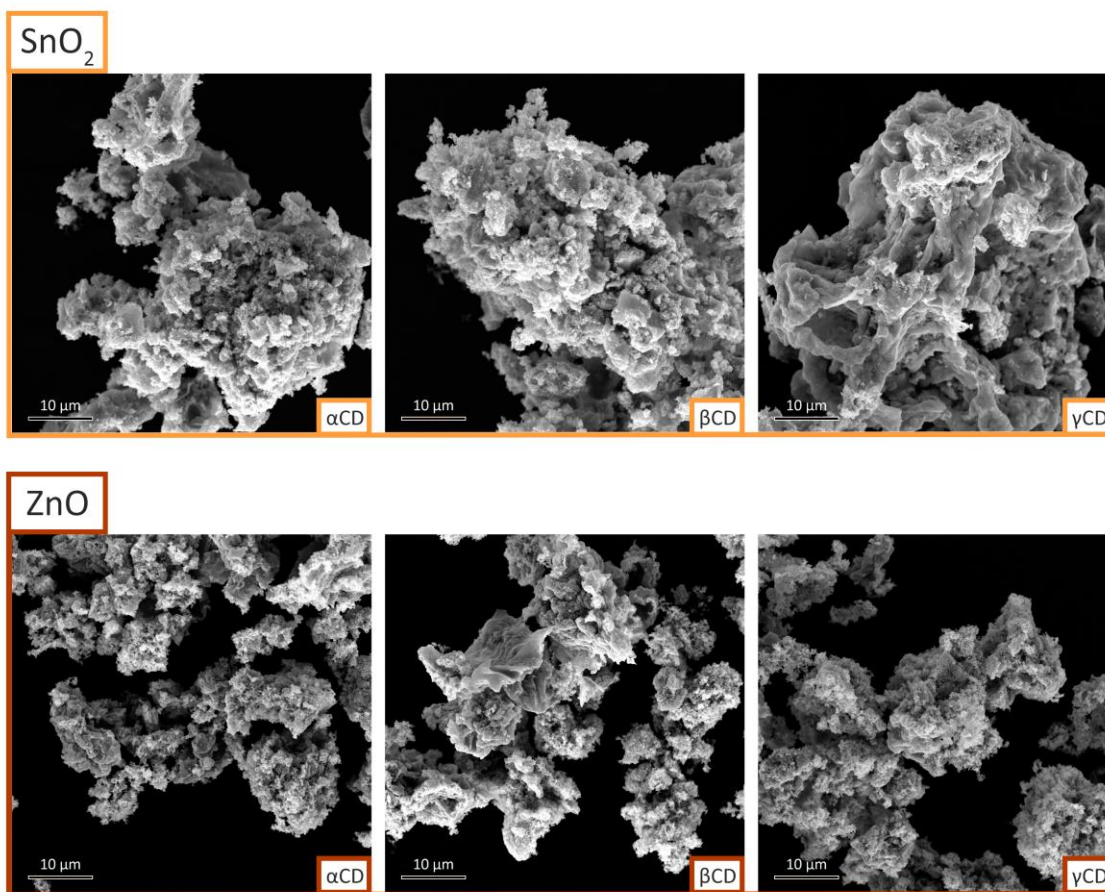
283 Moreover, a less effective protective effect can also be hypothesized from an analysis of the TG
284 curves reported in inset b) of Figure 3: in the area around 400 degrees, where in presence of oxygen
285 presumably occurs the oxidation/combustion of the cyclodextrins, it is possible to notice an
286 anomalous behavior (very evident in the peaks of the first derivative). These small weight losses
287 can be related to volatiles that are quickly released as soon as the protective "cage" is thermally
288 oxidized. Given the tendency of ZnAc to sublime, reported in the literature, it can be
289 hypothesized that part of the precursor is actually not converted but rather simply "blocked" and
290 subsequently lost during the heating.

291 Another plausible reason in the different superficial area from a comparison of the two different
292 precursors can be related to the fact that in the case of the SnO₂, the kneading phase is carried out
293 with a liquid precursor, tin (II) 2-ethylhexanoate, instead of a powder such as in the case of the
294 Zinc Acetate: the liquid form of the precursor leads to a much more effective grinding / mixing,

295 leading to the obtainment of a sort of "paste". From a practical point of view, the kneading phase
296 therefore seems to have a significant influence on the final result.

297

298 We also characterized the final oxides from the morphological point of view by scanning electron
299 microscopy, results are shown below (Figure 4):



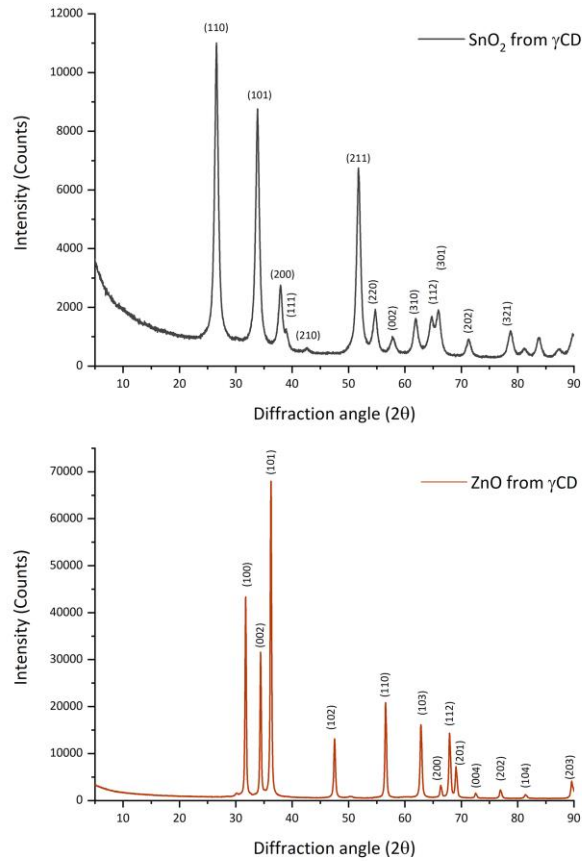
300

301 **Figure 4 SEM images of the oxide obtained from different precursors and CDs. Instrumental magnification**
302 **5kx, 10keV**

303

304 The suitable temperatures for calcining the mixture after the kneading step were chosen on the
305 results obtained by TG analyses, considering the temperatures at which the weight losses are
306 concluded: the same temperature, 500 °C was, used for the calcination of all kneaded mixtures,

307 leading to a white and uniform oxide residue. As shown in Figure 4, there are no particular
308 differences that emerge from the SEM comparison of the samples, even if obtained from different
309 mixtures of oxides and oligomers. Higher magnification are reported in Supporting Informations.



310

311 **Figure 5 XRD patterns of SnO₂ and ZnO, from precursot/γCD mixtures.**

312 The XRD confirms that the samples are constituted by crystalline cassiterite (SnO₂ in the
313 tetragonal crystal phase, JCPDS file number 00-001-0625). The calculated size (D, via Debye-
314 Sherrer equation) is

315 TEM

316 CONCLUSIONS

317

318

319

320

321 CORRESPONDING AUTHOR

322 *alberto.rubinpedrazzo@unito.it, Post-Doc Fellow

323 ABBREVIATIONS

324 α CD, alpha-cyclodextrin; β CD, beta-cyclodextrin; γ CD, gamma-cyclodextrin; BM, ball-mill;

325 SnEx, Tin(II) 2-ethylhexanoate; ZnAc, Zinc Acetate;

326

327

328

329 REFERENCES

330 (1) Bracco, P., Scalarone, D., Trotta, F. Electrospun Membranes for Sensors Applications, in:
331 Smart Membranes and Sensors: Synthesis, Characterization, and Applications. *Ed.*
332 *Scrivener Publ.* **2014**, 301–336.

333 (2) Eranna, G.; Joshi, B. C.; Runthala, D. P.; Gupta, R. P. Oxide Materials for Development of
334 Integrated Gas Sensors - A Comprehensive Review. *Crit. Rev. Solid State Mater. Sci.* **2004**,
335 *29* (3–4), 111–188. <https://doi.org/10.1080/10408430490888977>.

336 (3) Sun, Y.-F.; Liu, S.-B.; Meng, F.-L.; Liu, J.-Y.; Jin, Z.; Kong, L.-T.; Liu, J.-H. Metal Oxide
337 Nanostructures and Their Gas Sensing Properties: A Review. *Sensors* **2012**, *12* (12), 2610–
338 2631. <https://doi.org/10.3390/s120302610>.

339 (4) Zaera, F. Nanostructured Materials for Applications in Heterogeneous Catalysis. *Chem.*
340 *Soc. Rev.* **2013**, *42* (7), 2746–2762. <https://doi.org/10.1039/C2CS35261C>.

341 (5) Yu, X.; Marks, T. J.; Facchetti, A. Metal Oxides for Optoelectronic Applications. *Nat. Publ.*
342 *Gr.* **2016**, *15* (4), 383–396. <https://doi.org/10.1038/nmat4599>.

- 343 (6) Das, S.; Jayaraman, V. SnO₂: A Comprehensive Review on Structures and Gas Sensors.
344 *Prog. Mater. Sci.* **2014**, *66*, 112–255. <https://doi.org/10.1016/j.pmatsci.2014.06.003>.
- 345 (7) Li, D.; Xia, Y. Fabrication of Titania Nanofibers by Electrospinning. *Nano Lett.* **2003**, *3*
346 (4), 555–560. <https://doi.org/10.1021/nl034039o>.
- 347 (8) Choi, S. S.; Lee, S. G.; Im, S. .; Kim, S. H.; Joo, Y. L. Silica Nanofibers from
348 Electrospinning/Sol-Gel Process. *J. Mater Sci. Lett.* **2003**, *22* (12), 891–893.
- 349 (9) Morandi, S.; Cecone, C.; Marchisio, G.; Bracco, P.; Zanetti, M.; Manzoli, M. Shedding
350 Light on Precursor and Thermal Treatment Effects on the Nanostructure of Electrospun
351 TiO₂ Fibers. *Nano-Structures and Nano-Objects* **2016**, *7*, 49–55.
352 <https://doi.org/10.1016/j.nanoso.2016.05.003>.
- 353 (10) Chandraiah, M.; Sahoo, B.; Panda, P. K. Preparation and Characterization of SnO₂
354 Nanofibers by Electrospinning. *Trans. Indian Ceram. Soc.* **2014**, *73* (4), 266–269.
355 <https://doi.org/Doi 10.1080/0371750x.2014.923786>.
- 356 (11) Madhugiri, S.; Sun, B.; Smirniotis, P. G.; Ferraris, J. P.; Balkus, K. J. Electrospun
357 Mesoporous Titanium Dioxide Fibers. *Microporous Mesoporous Mater.* **2004**, *69* (1–2),
358 77–83. <https://doi.org/10.1016/j.micromeso.2003.12.023>.
- 359 (12) Bazargan, A. M.; Fateminia, S. M. A.; Ganji, M. E.; Bahrevar, M. A. Electrospinning
360 Preparation and Characterization of Cadmium Oxide Nanofibers. *Chem. Eng. J.* **2009**, *155*
361 (1–2), 523–527. <https://doi.org/10.1016/j.cej.2009.08.004>.
- 362 (13) Dai, Y.; Liu, W.; Formo, E.; Sun, Y.; Xia, Y. Ceramic Nanofibers Fabricated by
363 Electrospinning and Their Applications in Catalysis, Environmental Science, and Energy
364 Technology. *Polym. Adv. Technol.* **2011**, *22* (3), 326–338. <https://doi.org/10.1002/pat.1839>.
- 365 (14) Masa, S.; Hontanon, E.; Santos, J. P.; Sayago, I.; Lozano, J. Chemiresistive Sensors Based
366 on Electrospun Tin Oxide Nanofibers for Detecting NO₂ at the Sub-0.1 Ppm Level. *Proc.*
367 *2019 5th Exp. Int. Conf. exp.at 2019, 2019, Funchal, Madeira Island, Port.* **2019**, No. 2,
368 310–314. <https://doi.org/10.1109/EXPAT.2019.8876485>.

- 369 (15) MacDiarmid, A. G.; Jones, W. .; Norris, J. D.; Gao, J.; Johnson, A. T.; Pinto, N. J.; Hone,
370 J.; Han, F. K. Electrostatically-Generated Nano Fibers of Electronic Polymers. *Synth. Met.*
371 **2001**, *119* (1–3), 27–30.
- 372 (16) Theron, S. A.; Zussman, E.; Yarin, A. L. Experimental Investigation of the Governing
373 Parameters in the Electrospinning of Polymer Solutions. **2004**, *45* (2004), 2017–2030.
374 <https://doi.org/10.1016/j.polymer.2004.01.024>.
- 375 (17) Liu, S.; White, K. L.; Reneker, D. H. Electrospinning Polymer Nanofibers with Controlled
376 Diameters. *IEEE Trans. Ind. Appl.* **2019**, *55* (5), 5239–5243.
377 <https://doi.org/10.1109/TIA.2019.2920811>.
- 378 (18) Rubin Pedrazzo, A.; Cecone, C.; Morandi, S.; Manzoli, M.; Bracco, P.; Zanetti, M.
379 Nanosized SnO₂ Prepared by Electrospinning: Influence of the Polymer on Both
380 Morphology and Microstructure. *Polymers (Basel)*. **2021**, *13* (6).
381 <https://doi.org/10.3390/polym13060977>.
- 382 (19) Fioravanti, A.; Morandi, S.; Rubin Pedrazzo, A.; Bracco, P.; Zanetti, M.; Manzoli, M.;
383 Mazzocchi, M.; Carotta, M. C. Ultrasensitive Gas Sensors Based on Electrospun TiO₂ and
384 ZnO. *Proceedings* **2017**, *1* (4), 485. <https://doi.org/10.3390/proceedings1040485>.
- 385 (20) Wang, X.; Fan, H.; Ren, P. Electrospinning Derived Hollow SnO₂ Microtubes with Highly
386 Photocatalytic Property. *Catal. Commun.* **2013**, *31*, 37–41.
387 <https://doi.org/10.1016/j.catcom.2012.11.009>.
- 388 (21) Sun, X.; Huang, Y.; Zong, M.; Wu, H.; Ding, X. Preparation of Porous SnO₂/ZnO
389 Nanotubes via a Single Spinneret Electrospinning Technique as Anodes for Lithium Ion
390 Batteries. *J. Mater. Sci. Mater. Electron.* **2016**, *27* (3), 2682–2686.
391 <https://doi.org/10.1007/s10854-015-4077-x>.
- 392 (22) Sun, Y.; Wang, J.; Du, H.; Li, X.; Wang, C.; Hou, T. Formaldehyde Gas Sensors Based on
393 SnO₂/ZSM-5 Zeolite Composite Nanofibers. *J. Alloys Compd.* **2021**, *868*, 159140.
394 <https://doi.org/10.1016/j.jallcom.2021.159140>.
- 395 (23) Kurkov, S. V.; Loftsson, T. Cyclodextrins. *Int. J. Pharm.* **2013**, *453* (1), 167–180.

- 396 <https://doi.org/10.1016/j.ijpharm.2012.06.055>.
- 397 (24) Duchêne, D. Cyclodextrins and Their Inclusion Complexes. *Cyclodextrins Pharm. Cosmet.*
398 *Biomed. Curr. Futur. Ind. Appl.* **2011**, 1–18. <https://doi.org/10.1002/9780470926819.ch1>.
- 399 (25) Szejtli, J. Introduction and General Overview of Cyclodextrin Chemistry. *Chem. Rev.* **1998**,
400 *98* (5), 1743–1754. <https://doi.org/10.1021/cr970022c>.
- 401 (26) Szejtli, J. Utilization of Cyclodextrins in Industrial Products and Processes. *J. Mater. Chem.*
402 **1997**, *7* (4), 575–587. <https://doi.org/10.1039/a605235e>.
- 403 (27) Loftsson, T.; Duchêne, D. Cyclodextrins and Their Pharmaceutical Applications. *Int. J.*
404 *Pharm.* **2007**, *329* (1–2), 1–11. <https://doi.org/10.1016/j.ijpharm.2006.10.044>.
- 405 (28) Szejtli, J. *Cyclodextrin Technology*; s.l.:Springer Netherlands, 1988.
- 406 (29) Marques, H. M. C. A Review on Cyclodextrin Encapsulation of Essential Oils and Volatiles.
407 *Flavour Fragr. J.* **2010**, *25* (5), 313–326. <https://doi.org/10.1002/ffj.2019>.
- 408 (30) Saenger, W. Cyclodextrin Inclusion Compounds in Research and Industry. *Angew. Chemie*
409 *Int. Ed. English* **1980**, *19* (5), 344–362. <https://doi.org/10.1002/anie.198003441>.
- 410 (31) Prochowicz, D.; Kornowicz, A.; Lewiński, J. Interactions of Native Cyclodextrins with
411 Metal Ions and Inorganic Nanoparticles: Fertile Landscape for Chemistry and Materials
412 Science. *Chem. Rev.* **2017**, *117* (22), 13461–13501.
413 <https://doi.org/10.1021/acs.chemrev.7b00231>.
- 414 (32) Norkus, E. Metal Ion Complexes with Native Cyclodextrins. An Overview. *J. Incl. Phenom.*
415 *Macrocycl. Chem.* **2009**, *65* (3), 237–248. <https://doi.org/10.1007/s10847-009-9586-x>.
- 416 (33) Erem Bilensoy. *Cyclodextrins in Pharmaceuticals, Cosmetics, and Biomedicine: Current and*
417 *Future Industrial Applications*; John Wiley and Sons Inc, Ed.; 2011.
- 418 (34) Zhang, J.; Xu, D.; Qian, W.; Zhu, J.; Yan, F. Host-Guest Inclusion Complexes Derived
419 Heteroatom-Doped Porous Carbon Materials. *Carbon N. Y.* **2016**, *105*, 183–190.
420 <https://doi.org/10.1016/j.carbon.2016.04.034>.

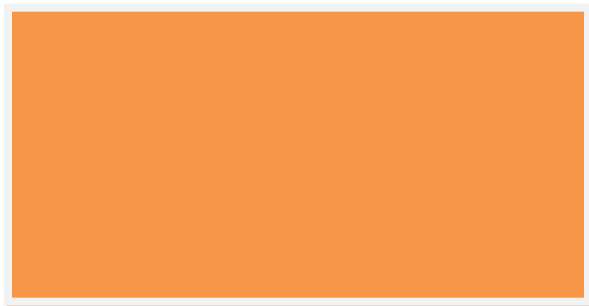
- 421 (35) Q. Qi, T. Zhang, L. L. and X. Z. Synthesis and Toluene Sensing Properties of SnO₂
422 Nanofibers. *Sensors Actuators B Chem.* **2009**, *137*, 471.
- 423 (36) Wang, W.; Huang, H.; Li, Z.; Zhang, H.; Wang, Y.; Zheng, W.; Wang, C. Zinc Oxide
424 Nanofiber Gas Sensors via Electrospinning. *J. Am. Ceram. Soc.* **2008**, *91* (11), 3817–3819.
425 <https://doi.org/10.1111/j.1551-2916.2008.02765.x>.
- 426 (37) Anastas, P. T.; Warner, J. C. *Green Chemistry: Theory and Practice*; Oxford University
427 Press, 1998.
- 428 (38) Anastas, P. T.; Zimmerman, J. B. Design through the 12 Principles of Green Engineering.
429 *IEEE Eng. Manag. Rev.* **2007**, *35* (3), 16. <https://doi.org/10.1109/EMR.2007.4296421>.
- 430 (39) Verma, S.; Rawat, A.; Kaul, M.; Saini, S. Solid Dispersion: A Strategy for Solubility
431 Enhancement. *Int. J. Pharm. Technol.* **2011**, *3* (2), 1062–1099.
- 432 (40) Patil, J. S.; Kadam, D. V.; Marapur, S. C.; Kamalapur, M. V. Inclusion Complex System; a
433 Novel Technique to Improve the Solubility and Bioavailability of Poorly Soluble Drugs: A
434 Review. *Int. J. Pharm. Sci. Rev. Res.* **2010**, *2* (2), 29–34.
- 435 (41) Crini, G. Recent Developments in Polysaccharide-Based Materials Used as Adsorbents in
436 Wastewater Treatment. *Prog. Polym. Sci.* **2005**, *30* (1), 38–70.
437 <https://doi.org/10.1016/j.progpolymsci.2004.11.002>.
- 438 (42) Loftsson, T.; Saokham, P.; Sá Couto, A. R. Self-Association of Cyclodextrins and
439 Cyclodextrin Complexes in Aqueous Solutions. *Int. J. Pharm.* **2019**, *560* (5), 228–234.
440 <https://doi.org/10.1016/j.ijpharm.2019.02.004>.
- 441 (43) Loftsson, T.; Magnúsdóttir, A.; Másson, M.; Sigurjónsdóttir, J. F. Self-Association and
442 Cyclodextrin Solubilization of Drugs. *J. Pharm. Sci.* **2002**, *91* (11), 2307–2316.
443 <https://doi.org/10.1002/jps.10226>.
- 444 (44) Mazzaglia, A.; Sciortino, M. T.; Kandoth, N.; Sortino, S. Cyclodextrin-Based
445 Nanoconstructs for Photoactivated Therapies. *J. Drug Deliv. Sci. Technol.* **2012**, *22* (3),
446 235–242. [https://doi.org/10.1016/S1773-2247\(12\)50034-1](https://doi.org/10.1016/S1773-2247(12)50034-1).

- 447 (45) Zhang, J.; Ma, P. X. Cyclodextrin-Based Supramolecular Systems for Drug Delivery:
448 Recent Progress and Future Perspective. *Adv. Drug Deliv. Rev.* **2013**, *65* (9), 1215–1233.
449 <https://doi.org/10.1016/j.addr.2013.05.001>.
- 450 (46) Brochsztain, S.; Politi, M. J. Solubilization of 1,4,5,8- Naphthalenediimides and 1, 8-
451 Naphthalimides through the Formation of Novel Host–Guest Complexes with a-
452 Cyclodextrin. *Langmuir* **1999**, *15*, 486–4494.
- 453 (47) Mar, G. L.; Timbrell, P. Y.; Lamb, R. N. Formation of Zinc Oxide Thin Films by the
454 Thermal Decomposition of Zinc Acetate. **1993**, *73*, 177–192. [https://doi.org/10.1007/978-](https://doi.org/10.1007/978-3-642-84933-6_15)
455 [3-642-84933-6_15](https://doi.org/10.1007/978-3-642-84933-6_15).
- 456 (48) Trotta, F.; Zanetti, M.; Camino, G. Thermal Degradation of Cyclodextrins. **2000**, *69*, 373–
457 379.

458

459 TOC/GRAPHIC ABSTRACT

460



461

462

463

464

465 SYNOPSIS